L. Susmel, Frattura ed Integrità Strutturale, 16 (2011) 5-17; DOI: 10.3221/IGF-ESIS.16.01

On the overall accuracy of the Modified Wöhler Curve Method in estimating high-cycle multiaxial fatigue strength

Luca Susmel
Department of Engineering, University of Ferrara, Via Saragat, 1 – 44100 Italy
Department of Mechanical Engineering, Trinity College, Dublin 2, Ireland
Department of Civil and Structural Engineering, University of Sheffield, Mappin Street, Sheffield, S1 3JD, UK
ssl@unife.it

ABSTRACT. The aim of the present paper is to systematically investigate the accuracy of the so-called Modified Wöhler Curve Method (MWCM) in estimating high-cycle fatigue strength of plain and notched engineering materials damaged by in-service multiaxial load histories. In more detail, the MWCM, which is a bi-parametrical critical plane approach, postulates that initiation and Stage I propagation of fatigue cracks occur on those material planes experiencing the maximum shear stress amplitude (this being assumed to be always true independently from the degree of multiaxiality of the applied loading path). Further, the fatigue damage extent is hypothesised to depend also on the maximum stress perpendicular to the critical plane, the mean normal stress being corrected through the so-called mean stress sensitivity index (i.e., a material constant capable of quantifying the sensitivity of the assessed material to the presence of superimposed static stresses). In the present investigation, the overall accuracy of the MWCM in estimating high-cycle fatigue strength was checked through 704 endurance limits taken from the literature and generated, under multiaxial fatigue loading, by testing both plain and notched samples made of 71 different materials. Such a massive validation exercise allowed us to prove that the MWCM is highly accurate, resulting in 95% of the estimates falling within an error interval equal to ±15%.

KEYWORDS. Multiaxial fatigue; Critical plane approach; High-cycle fatigue strength; Notch.

INTRODUCTION

Since the pioneering work done by Gough [1], over the last 60 years several researchers have made a big effort in order to devise sound criteria allowing high-cycle fatigue damage under multiaxial fatigue loading to be estimated accurately. As to the work that has been done so far, examination of the state of the art shows that the most important high-cycle fatigue criteria can be subdivided into the following three different groups: methods making use of the so-called microscopic approach [2, 3], fatigue assessment techniques based on the use of the stress invariants [4-6], and, finally, criteria taking full advantage of the classical critical plane concept [7-9]. Amongst the above different strategies, it is the author's opinion that the most promising approaches are those based on the assumption that fatigue damage reaches its maximum value on that material plane (i.e., the so-called critical plane) experiencing the maximum shear stress amplitude [10]. According to the above firm belief, over the last decade we have made a big effort in order to systematically investigate the peculiarities of a bi-parametrical critical plane approach which is known as the Modified

Wöhler Curve Method (MWCM) [11]. In more detail, initially we checked the accuracy and reliability of such a criterion in estimating both high-cycle fatigue damage [12, 13] and lifetime [14, 15] of plain engineering materials subjected to multiaxial fatigue loading. Subsequently, attention has been focused on the problem of estimating multiaxial fatigue damage in the presence of stress concentration phenomena [16-19], by also investigating the related problem of designing welded connections against multiaxial fatigue [20-24].
Recently, basing his investigation on several experimental results taken from the literature, Jan Papuga [25] has performed a systematic comparison amongst different criteria in order to select the most accurate one in estimating high-cycle fatigue damage in plain engineering materials subjected to multiaxial loading paths. According to his calculations, he has come to the conclusion that the use of the MWCM results in poor estimates, especially when superimposed static stresses are involved. In our opinion, such an erroneous conclusion has to be ascribed to the fact that Dr. Papuga has applied our approach in a wrong way, by systematically miscalculating the stress quantities relative to the critical planes. Accordingly, in the present paper the main features of the MWCM are initially reviewed by focusing attention mainly on the problem of determining the so-called mean stress sensitivity index. Subsequently, it is proven, through 704 experimental endurance limits generated by testing both plain and notched samples made of 71 different materials, that, when the MWCM is used correctly, it is capable of estimates falling mainly within an error interval of ±10%.

FUNDAMENTALS OF THE MWCM

The MWCM is a critical plane approach which estimates multiaxial fatigue damage through the maximum shear stress amplitude, τ_a, as well as through the mean value, $\sigma_{n,m}$, and the amplitude, $\sigma_{n,a}$, of the stress perpendicular to the critical plane. According to the fatigue damage model the MWCM is based on [11], the critical plane is defined as that material plane experiencing the maximum shear stress amplitude, τ_a. From a practical point of view, the combined effect of both τ_a, $\sigma_{n,m}$ and $\sigma_{n,a}$ are taken into account simultaneously through the following stress index [13]:

$$\rho_{eff} = \frac{m \cdot \sigma_{n,m} + \sigma_{n,a}}{\tau_a} \tag{1}$$

In the above identity, mean stress sensitivity index m [13] is a material property to be determined experimentally whose main features will be investigated in the next section in great detail. As to ratio ρ_{eff} instead, thanks the way it is defined, such a stress index is seen to be sensitive not only to the presence of superimposed static stresses, but also to the degree of non-proportionality of the applied loading path [11].
Turning back to the MWCM, the way it estimates fatigue damage under multiaxial fatigue loading is schematically shown by the modified Wöhler diagram reported in Fig. 1a. The above log-log diagram plots the shear stress amplitude relative to the critical plane, τ_a, against the number of cycles to failure, N_f. By performing a systematic reanalysis based on numerous experimental data [12, 14, 15], it was proven that, as index ρ_{eff} varies, different fatigue curves are obtained (Fig. 1a). In particular, it was observed that fatigue damage tends to increase as ρ_{eff} increases: this results in the fact that the corresponding fatigue curve tends to shift downward in the above diagram with increasing of ρ_{eff} (Fig. 1a). According to the classical log-log schematisation used to summarise fatigue data, the position and the negative inverse slope of any Modified Wöhler curve can unambiguously be defined through the following linear relationships [11, 12, 15]:

$$k_\tau(\rho) = \alpha \cdot \rho + \beta \tag{2}$$

$$\tau_{\mathrm{Re}f}(\rho) = a \cdot \rho + b \tag{3}$$

In the above definitions, $k_\tau(\rho_{eff})$ is the negative inverse slope, while $\tau_{Ref}(\rho_{eff})$ is the reference shear stress amplitude extrapolated at N_A cycles to failure (see Fig. 1a). Further, α, β, a and b are material constants to be determined experimentally. In particular, by remembering that ρ_{eff} is equal to unity under fully-reversed loading and to zero under torsional loading [11], constants a and b in Eq. (3) can be calculated directly as follows:

$$\tau_{\mathrm{Re}f}(\rho_{eff}) = \left(\frac{\sigma_A}{2} - \tau_A\right) \cdot \rho_{eff} - \tau_A, \tag{4}$$

where σ_A and τ_A are the endurance limits extrapolated at N_A cycles to failure under fully-reversed uniaxial and torsional fatigue loading, respectively.
When our criterion is specifically used to estimate high-cycle fatigue damage, according to the MWCM's philosophy, a material is at the endurance limit condition when the amplitude of the shear stress relative to the critical plane, τ_a, equals the reference shear stress estimated, through Eq. (3), for the pertinent value of ratio ρ_{eff}, that is [11]:

$$\tau_a \le \tau_{Ref}(\rho_{eff}) = \left(\frac{\sigma_A}{2} - \tau_A\right)\cdot\rho_{eff} + \tau_A \Rightarrow$$
$$\Rightarrow \tau_{A,eq} = \tau_a - \left(\frac{\sigma_A}{2} - \tau_A\right)\cdot\rho_{eff} \le \tau_A \qquad (6)$$

If the above equation is plotted in a τ_a vs. ρ_{eff} diagram (Fig. 1b), it is straightforward to see that, given the value of ρ_{eff}, fatigue breakage should not occur up to a number of cycles to failure equal to N_A as long as the shear stress amplitude relative to the critical plane is below the limit curve determined according to the criterion itself.

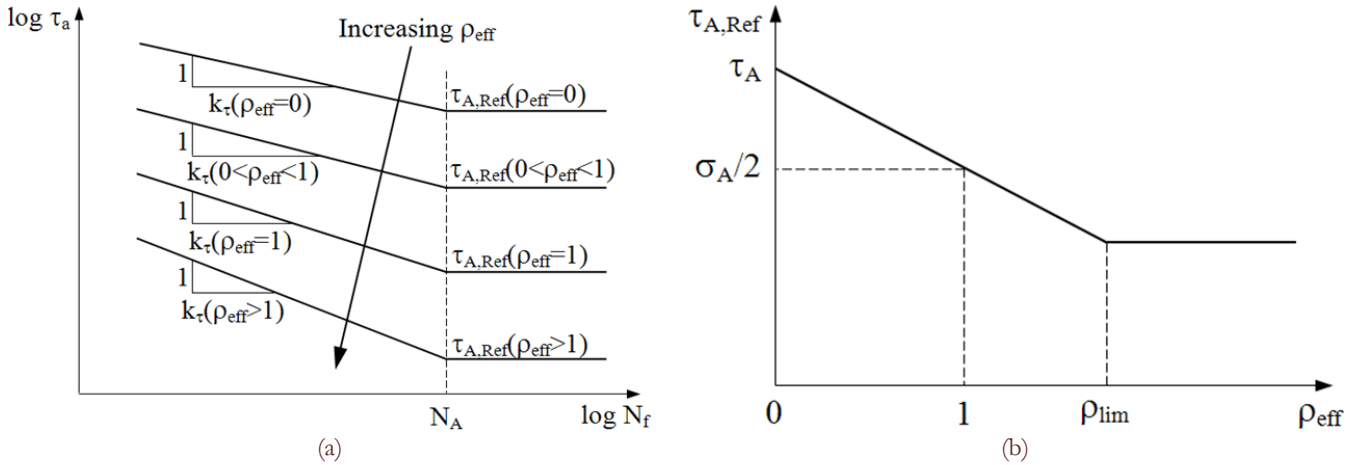

Figure 1: Modified Wöhler diagram (a) and adopted correction for the $\tau_{A,Ref}$ vs. ρ_{eff} relationship (b).

To conclude, it is worth observing that, as shown by the above chart, the reference shear stress to be used to estimate multiaxial fatigue damage is assumed to be constant and equal to $\tau_{Ref}(\rho_{lim})$ for ρ_{eff} larger than limit value ρ_{lim} [11, 13]. This correction, which plays a fundamental role in the overall accuracy of the MWCM, was introduced in light of the fact that, under large values of ratio ρ_{eff}, the predictions made by the MWCM were seen to become too conservative [26]. According to the experimental results due to Kaufman and Topper [27], such a high degree of conservatism was ascribed to the fact that, when micro/meso cracks are fully open, an increase of the normal mean stress does not result in a further increase of fatigue damage. Therefore, by taking full advantage of the intrinsic mathematical limit of Eq. (6), which becomes evident when our criterion is directly expressed in terms of τ_a and $\sigma_{n,max}=\sigma_{n,a}+\sigma_{n,m}$ [11, 13], ρ_{lim} takes on the following value:

$$\rho_{lim} = \frac{\tau_A}{2\tau_A - \sigma_A} \qquad (7)$$

DETERMINING THE MEAN STRESS SENSITIVITY INDEX

In order to address the problem of estimating mean stress sensitivity index m, initially, it is useful to define the load ratio relative to the critical plane, R_{CP}, as follows [13]:

$$R_{CP} = \frac{\sigma_{n,min}}{\sigma_{n,max}} \qquad (8)$$

where $\sigma_{n,min}$ and $\sigma_{n,max}$ denote the minimum and the maximum value of the stress perpendicular to the plane of maximum shear stress amplitude, respectively.
In order to estimate mean stress sensitivity index m, assume now that endurance limits σ_A and τ_A are known from the experiments, so that, the only unknown material property in Eq. (6) is m itself. By observing now that both σ_A and τ_A are material fatigue properties generated under fully-reversed loading (i.e., R_{CP}=-1), it is logical to argue that material constant m has to be estimated from a third endurance limit determined under a value of R_{CP} larger than -1. Accordingly, if τ_a^*, $\sigma_{n,m}^*$ and $\sigma_{n,a}^*$ are the critical plane stress components referred to the above endurance limit condition, by rearranging Eq. (6), it is trivial to derive the following identity [11, 19]:

$$m = \frac{\tau_a^*}{\sigma_{n,m}^*}\left(2\frac{\tau_A - \tau_a^*}{2\tau_A - \sigma_A} - \frac{\sigma_{n,a}^*}{\tau_a^*}\right) \tag{9}$$

which allows m to be calculated directly. As to the expected values for m, it can be said that, since m quantifies the portion of the mean normal stress relative to the critical plane which effectively opens the micro/meso cracks by favouring their propagation [11], such a material fatigue property is expected to vary in the range 0-1: when m is equal to unity, the material being assessed is assumed to be fully sensitive to the mean stress perpendicular to the critical plane; on the contrary, an m value equal to zero implies that the investigated material is not sensitive at all to the presence of superimposed static tensile stresses.
With regard to the estimation of the mean stress sensitivity index, it is not superfluous to notice here that, in situations of practical interest, the above material constant can easily be determined by directly using a uniaxial endurance limit generated under a load ratio, $R=\sigma_{x,min}/\sigma_{x,max}$ (Fig. 2), larger than -1. In more detail, under axial or bending fatigue loading with superimposed static stress, it is straightforward to see that the relevant stress quantities relative to the critical plane take on the following values [11]:

$$\tau_a = \sigma_{n,a} = \frac{\sigma_{x,a}}{2};\ \sigma_{n,m} = \frac{\sigma_{x,m}}{2} \tag{10}$$

where $\sigma_{x,a}$ and $\sigma_{x,m}$ are the amplitude and the mean value of the applied stress, respectively.

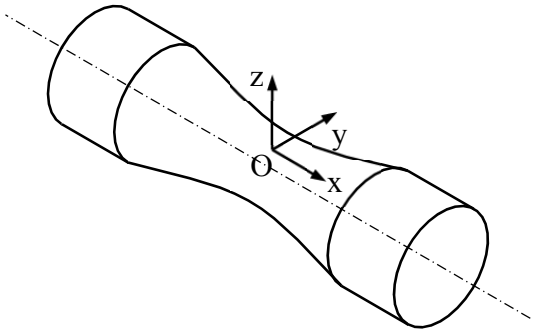

Figure 2: Cylindrical specimen and adopted frame of reference.

From a physical point of view, the meaning of mean stress sensitivity index m can be explained by taking full advantage of the outcomes summarised by Kaufman and Topper in Ref. [27]. In more detail, by performing an accurate experimental investigation they have observed that, when the mean stress perpendicular to the Stage I planes is larger than a certain material threshold value, an increase of the mean stress itself does not result in any further increase of fatigue damage. This experimental evidence was ascribed by Kaufman and Topper themselves to the fact that, in the presence of large values of the mean stress perpendicular to the growth direction, micro/meso shear cracks are already fully open, so that, the shearing forces are directly transmitted to the crack tips by favouring the Mode II growth. On the contrary, when the mean stress normal to the Stage I planes is lower than the above material threshold value, the effect of the shearing forces pushing the crack tips is reduced due to the interactions amongst the asperities characterising the two faces of the cracks themselves. Since the microstructure morphology varies from material to material by resulting in a different roughness of

the crack faces, it is logical to presume that the value of the mean stress sensitivity index changes as the microstructural features of the material being assessed vary.
To conclude, it is worth observing that not only to estimate m correctly but also to apply the MWCCM properly, a multi-parameter optimisation process has to be run to unambiguously determine the orientation of the critical plane [28]. As to such a tricky aspect of the multiaxial fatigue issue, it has to be said that this laborious *modus operandi* is a direct consequence of the classical fatigue damage model on which the MWCM is based [11, 29]. In fact, independently from the complexity of the time-variable stress state damaging the material point at which the stress analysis is performed, there always exist two or more material planes experiencing the maximum shear stress amplitude, so that, amongst all the potential critical planes, the one which has to be used to calculate mean stress sensitivity index m as well as to perform the fatigue assessment is the plane experiencing the largest value of the maximum normal stress.

VALIDATION BY EXPERIMENTAL RESULTS

In order to show the accuracy of the MWCM in estimating high-cycle fatigue strength under multiaxial fatigue loading, a systematic bibliographical investigation was carried out to select an appropriate set of fatigue results. In more detail, initially attention was focused on multiaxial endurance limits generated by testing un-notched samples. In the most general case, the applied loading paths included in-phase and out-of-phase situations (combined axial loading, bending, torsion and internal/external pressure) with and without superimposed static stresses, the applied stress components being defined as follows (see Fig. 2 for the adopted frame of reference):

$$\begin{aligned}\sigma_x(t) &= \sigma_{x,m} + \sigma_{x,a}\sin(\omega_x \cdot t)\\ \sigma_y(t) &= \sigma_{y,m} + \sigma_{y,a}\sin(\omega_y \cdot t + \delta_{y,x})\\ \tau_{xy}(t) &= \tau_{xy,m} + \tau_{xy,a}\sin\left(\omega_{xy} \cdot t + \delta_{xy,x}\right)\end{aligned} \tag{11}$$

In the above sinusoidal stress signals, subscript m and a denote the mean value and the amplitude of any stress components, respectively, ω_x, ω_y and ω_{xy} are the angular velocities, whereas $\delta_{y,x}$ and $\delta_{xy,x}$ are the out-of-phase angles, both measured with respect to signal $\sigma_x(t)$. Further, also a number of results generated under the complex loading paths sketched in Fig. 3 were considered in the validation exercise discussed in the present section. Tab. 1 summarises the static and fatigue properties of the materials of which the unnotched samples tested under multiaxial fatigue loading were made. Tab. 2 instead lists the experimental values of mean stress sensitivity index m for those materials having m lower than unity.

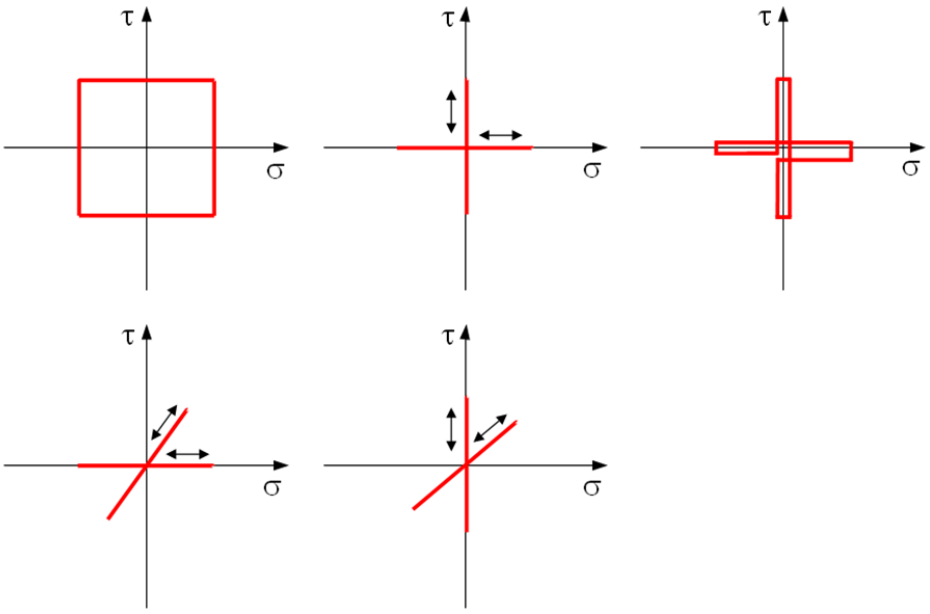

Figure 3: Investigated complex loading paths.

Material	Reference	σ_A [MPa]	τ_A [MPa]	σ_{UTS} [MPa]	Loding Path
0.1% C steel (normalised)	[1]	268.6	151.3	430.7	B-T
0.4% C steel (normalised)	[1]	331.9	206.9	648.4	B-T
0.4% C steel (spheroidized)	[1]	274.8	155.9	477.0	B-T
0.9% C steel (pearlitic)	[1]	352.0	240.8	847.5	B-T
3% Ni steel	[1]	342.7	205.3	526.4	B-T
3/3.5% Ni steel	[1]	444.7	267.1	722.5	B-T
Cr-Va steel	[1]	429.1	257.8	751.8	B-T
3.5% NiCr steel (n. impact)	[1]	540.3	352.0	895.3	B-T
3.5% NiCr steel (l. impact)	[1]	509.4	324.2	896.9	B-T
NiCrMo steel (60-70 tons)	[1]	602.1	337.7	1000.3	B-T
NiCrMo steel (75-80 tons)	[1]	660.7	342.7	1242.7	B-T
NiCr steel	[1]	772.3	452.3	1667.2	B-T
SILAL cast iron	[1]	240.8	219.2	240.9	B-T
NICROSILAL cast iron	[1]	253.2	211.5	256.8	B-T
S65A Steel	[30]	583.5	370.5	1000.8	B-T
Cast alloy steel	[30]	366.8	247.5	721.2	B-T
CuCr cast iron	[31]	251.0	198.6	445.4	B-T
Inoculated cast iron	[31]	177.9	157.2	321.3	B-T
NiCr cast iron	[31]	146.2	122.7	259.2	B-T
CrMo steel (Solid samples)	[32]	713.2	425.3	946.5	B-T
CrMo steel (Hollow samples)	[32]	688.9	412.8	946.5	B-T
CrMo steel	[32]	509.0	306.9	954.0	B-T
CrMo steel	[32]	589.6	367.6	944.8	B-T
CrMo steel	[32]	593.3	350.7	944.8	B-T
CrMo steel	[32]	628.3	366.6	954.0	B-T
NiCrMo steel S81	[32]	589.7	331.9	1103.8	B-T
NiCrMoVa steel	[32]	660.7	342.7	1242.7	B-T
CrMoVa steel DTD551	[32]	667.8	398.3	1397.1	B-T
CrMoVa steel DTD551	[32]	659.9	386.5	1397.1	B-T
CrMoVa steel DTD551	[32]	706.1	412.5	1368.7	B-T
CrMoVa steel DTD551	[32]	737.7	447.4	1368.7	B-T
NiCr steel (Solid samples)	[32]	666.7	369.7	1389.4	B-T
NiCr steel (Hollow samples)	[32]	653.2	339.6	1389.4	B-T
NiCr steel	[32]	771.9	452.3	1667.2	B-T
SAE 4340	[33]	462.0	286.0	-	B-T
Brass	[7]	83.4	73.6	319.8	B-T
High-strength steel	[7]	461.1	274.7	809.3	B-T
Nodular Cast Iron	[7]	196.2	186.4	476.8	B-T
Rolled Steel (Block D)	[7]	215.8	137.3	-	B-T
0.34% C steel	[34]	378.0	218.0	-	B-T
Carbon Steel	[35]	261.0	160.0	-	B-T

Table 1: (Caption on the next page).

Material	Reference	σ_A [MPa]	τ_A [MPa]	σ_{UTS} [MPa]	Loding Path
30NCD16 (Batch 1)	[36]	586.0	405.0	1160.0	B-T
30NCD16 (Batch 2)	[37]	660.0	410.0	1160.0	B-T
Cast Iron	[38]	151.0	92.0	-	IP-T
0.35% C Steel	[39]	216.0	142.0	559.0	IEP-Ax
Mild Steel	[40]	235.4	137.3	375.0	B-T
Hard Steel	[40]	313.9	196.2	680.0	B-T
3% C Cast Iron	[40]	96.1	91.2	180.9	B-T
Duraluminium	[40]	156.0	100.0	433.0	B-T
34Cr4	[41]	410.0	256.0	795.0	B-T
42CrMo4	[42]	398.0	267.0	1025.0	B-T
St35	[43]	206.0	123.0	395.0	IP-Ax-T
St35	[44]	230.0	130.0	-	IP-Ax
En24T	[45]	405.0	270.0	850.0	IP-Ax
XC18	[46]	332.0	186.0	520.0	B-T
34Cr4	[41]	343.0	204.0	710.0	IP-B-T
25CrMo4	[47]	340.0	228.0	780.0	B-T
Fe-Cu	[48]	319.0	220.0	-	B-T
25CrMo4	[49]	361.0	228.0	780.0	IP-B-T
Grey Cast Iron	[50]	164.0	124.7	278.8	B-T
CK45	[51]	423.0	287.0	-	B-T
FGS 800-2	[52]	294.0	220.0	815.0	B-T
FeE 460	[53]	272.0	174.0	670.0	Ax-T
FGS 700/2	[54]	294.0	218.0	750.0	B-T
Ti-6Al-4V	[55]	652.0	411.0	1090.0	B-T
High strength steel	[56]	630.0	364.0	-	B-T
High strength steel	[56]	298.0*	172.0	-	B-T
High strength steel	[56]	320.0	184.7*	-	B-T
R7T (Axial)	[57]	514.4*	297.0	820-940	Ax-T
R7T (Circum.)	[57]	537.0*	310.0	820-940	Ax-T
42CrMo4	[58]	525.7	336.3	996.0	Ax-T
39NiCrMo3	[59]	367.5	265.0	856	Ax-T
SAE 52100	[60]	866.0	540.0	2467.0	Ax-T
30NCD16	[61]	690.0	428.0	1200.0	B-T
GGG60	[62]	275.0	249.0	815.0	B-T
St60	[63]	294.0	176.0	765.0	IP-Ax
76S-T61	[64]	217.9	143.4	419.3	B-T
76S-T61	[64]	188.3	119.3	419.3	B-T
76S-T61	[64]	170.3	109.7	419.3	B-T
25CrMo4	[65]	340.0	228.0	801.0	IP-Ax-T
C35N	[66]	250.0	150.0	550.0	Ax-T
C35N	[67]	189.0	150.0	533.0	Ax-T

Table 1: Mechanical properties of the unnotched materials, where: *Estimated according to von Mises, Ax=axial loading, B=bending, T=torsion, I(E)P=internal (external) pressure.

Material	Reference	m
S65A Steel	[30]	0.41
42CrMo4	[42]	0.35
34Cr4	[41]	0.36
30NCD16 (Batch 2)	[37]	0.16
CK45	[51]	0.31
St35	[44]	0.29
30NCD16	[61]	0.64
St60	[63]	0.38
25CrMo4	[65]	0.89
En3B	[19]	0.22

Table 2: Values of the mean stress sensitivity index for those materials having m lower than unity.

The experimental fully-reversed torsional endurance limit, τ_A, vs. equivalent shear stress, $\tau_{A,eq}$, diagram reported in Fig. 4 summarises the accuracy of the MWCM in estimating the multiaxial endurance limits experimentally determined by testing unnotched samples made of 65 different metallic materials, the error being calculated as follows [68]:

$$Error\,[\%] = \frac{\tau_{A,eq} - \tau_A}{\tau_A} \cdot 100 \tag{12}$$

The above diagram makes it evident that the MWCM is highly accurate in estimating high-cycle fatigue strength of plain engineering materials subjected to multiaxial fatigue loading, resulting in 95% of the estimates falling within an error interval equal to ±15%.

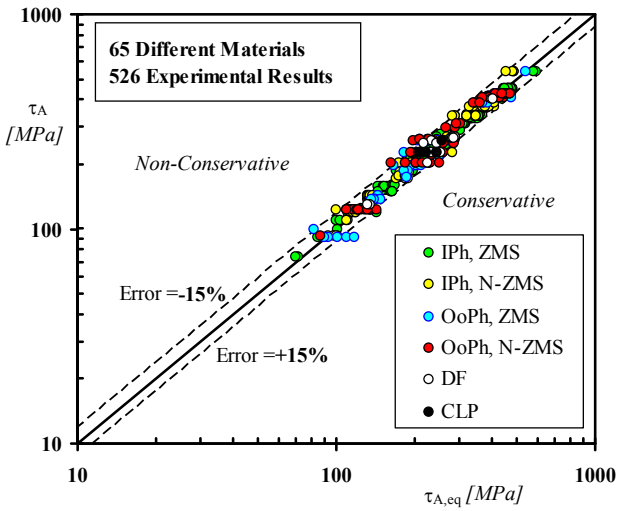

Figure 4: MWCM's accuracy in estimating high cycle fatigue strength of plain metallic materials subjected to multiaxial loading paths, where IPh=in-phase, OoPh=out-of-phase, ZMS=zero mean stress, N-ZMS=non-zero mean stress, DF=different frequences, CLP=complex loading paths (see Fig. 3).

In order to further investigate the accuracy of our multiaxial fatigue criterion, the MWCM was subsequently used, in terms of nominal stresses, to estimate high-cycle fatigue strength of notched samples subjected to in-phase and out-of-phase biaxial loading, by also considering situations involving non-zero mean stresses. Tab. 2 summarises the fully-reversed nominal uniaxial, σ_{An}, and torsional, τ_{An}, endurance limits of the considered notched samples, together with a brief description of the investigated geometrical features (see also Tab. 3 for the values of mean stress sensitivity index m). As to the notch endurance limits summarised in Tab. 2, it is worth observing that, since the uniaxial and torsional ones were not available for the notched samples of En3B [19], they have been estimated from the corresponding fatigue strength reduction factor, K_f, calculated according to Peterson's rule [73, 74].

The accuracy of the MWCM when applied in terms of nominal stresses in estimating high-cycle fatigue strength of notched components is summarised in the τ_{An} vs. $\tau_{A,eq}$ diagram reported in Fig. 5: the above chart makes it evident that the systematic use of our criterion resulted in 92% of the predictions falling within an error interval equal to ±15%.

Material	Ref.	σ_{An} [MPa]	τ_{An} [MPa]	Type of notched specimen
0.4% C Steel (Normalized)	[1]	179.1	176.0	V-notched cylindrical bar
3% Ni steel	[1]	209.9	151.3	V-notched cylindrical bar
3/3.5% Ni steel	[1]	302.6	183.7	V-notched cylindrical bar
Cr-Va steel	[1]	216.1	160.6	V-notched cylindrical bar
3.5% NiCr steel (n. impact)	[1]	268.6	236.2	V-notched cylindrical bar
3.5% NiCr steel (l. impact)	[1]	247.0	182.2	V-notched cylindrical bar
NiCrMo steel (75-80 tons)	[1]	271.7	240.8	V-notched cylindrical bar
CrMo steel	[32]	450.9	295.5	Cylindrical hollow sample with oil hole
CrMo steel	[32]	223.4	162.1	Cylindrical hollow sample with oil hole
CrMo steel	[32]	424.7	305.5	Cylindrical hollow sample with oil hole
CrMo steel	[32]	423.4	300.3	Cylindrical hollow sample with oil hole
CrMo steel	[32]	423.4	288.4	Cylindrical hollow sample with oil hole
NiCrMoVa steel	[32]	271.7	240.8	V-notched cylindrical bar
NiCrMoVa steel	[32]	288.7	211.5	Cylindrical hollow sample with oil hole
CrMoVa steel DTD551	[32]	300.7	235.4	Cylindrical hollow sample with oil hole
CrMoVa steel DTD551	[32]	297.8	220.9	Cylindrical hollow sample with oil hole
CrMoVa steel DTD551	[32]	471.3	354.6	Cylindrical hollow sample with oil hole
CrMoVa steel DTD551	[32]	448.1	354.9	Cylindrical hollow sample with oil hole
NiCr steel	[32]	312.5	225.5	Cylindrical hollow sample with oil hole
S65A steel	[30]	259.3	180.6	Cylindrical hollow sample with oil hole
S65A steel	[30]	347.3	270.1	Cylindrical shaft with fillet
S65A steel	[30]	563.5	185.2	Hollow specimens with 6 deep splines
16MnR	[69]	96.1	120.7	V-notched cylindrical bar
16MnR	[69]	174.3	155.3	V-notched cylindrical bar
SAE 1045	[70]	188.6	156.6	Cylindrical shaft with fillet
C40	[71]	117.8	152.8	V-notched cylindrical bar
CK45	[51]	311.8	220.4	Cylindrical shaft with fillet
Low Carbon Steel	[72]	66.9	122.7	V-notched cylindrical bar
Low Carbon Steel	[72]	95.3	156.4	V-notched cylindrical bar
En3B*	[19]	142.3	157.8	V-notched cylindrical bar
En3B*	[19]	204.7	211.3	V-notched cylindrical bar
En3B*	[19]	268.1	243.9	V-notched cylindrical bar
SAE 52100	[60]	631.0	539.0	V-notched cylindrical bar
SAE 52100	[60]	373.0	334.0	V-notched cylindrical bar

*Fully-reversed uniaxial and torsional endurance limits estimated according to Peterson.

Table 3: Fully-reversed uniaxial and torsional endurance limits for the investigated notched samples.

Finally, the diagram of Fig. 6 shows the error distribution measured in terms of Probability Density Function, which is nothing but the normal distribution calculated from the mean value and the standard deviation of any of the two considered data sets (i.e., plain and notched samples). In more detail, according to Fig. 6, the error distribution obtained when estimating multiaxial endurance limits of plain materials was characterised by a mean value equal to 0.3% and by a standard deviation of 7.3. Similarly, in the presence of stress concentration phenomena, the error distribution had mean value equal to -1.1% and standard deviation equal to 8.3. To conclude, it is possible to say that, as suggested by the Probability Density Function diagram of Fig. 6, the systematic use of the MWCM is seen to result in 85% of the estimates falling within an error interval of ±10%.

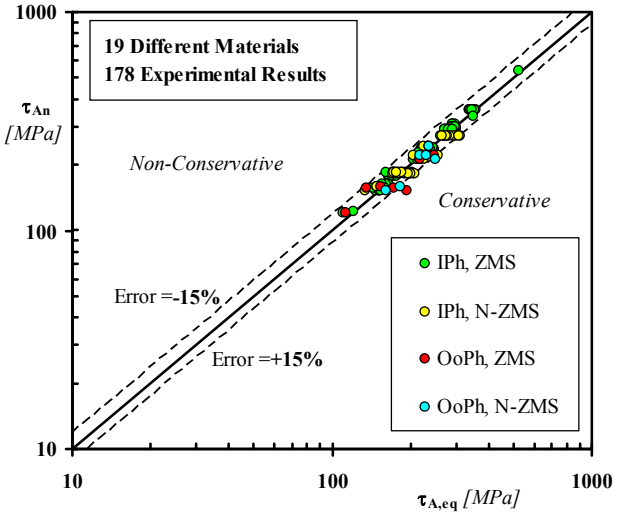

Figure 5: Accuracy of the MWCM, applied in terms of nominal stresses, in estimating high-cycle fatigue strength of notched metallic materials subjected to multiaxial loading paths, where IPh=in-phase, OoPh=out-of-phase, ZMS=zero mean stress, N-ZMS=non-zero mean stress.

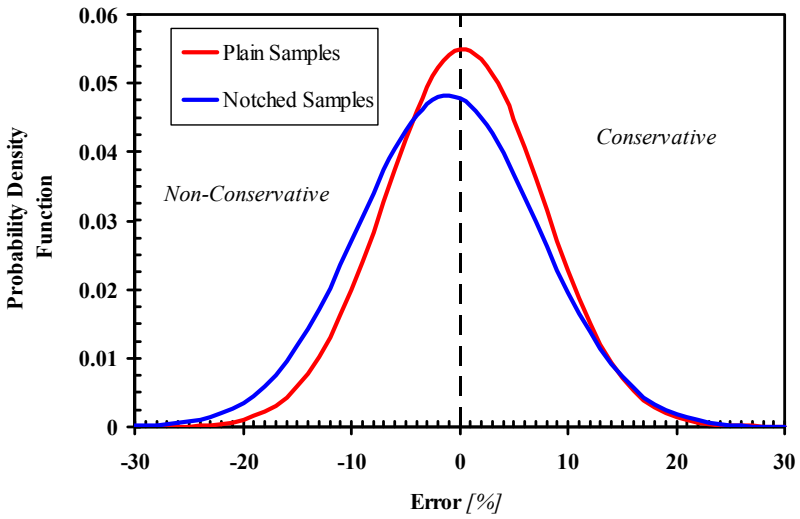

Figure 6: Error distribution in terms of Probability Density Function.

CONCLUSIONS

1) The MWCM is capable of correctly taking into account the mean stress effect in multiaxial fatigue;
2) The MWCM is seen to be highly accurate in accounting for the degree of multiaxiality and non-proportionality of the applied loading path;

3) Contrary to what stated by Dr. Papuga in Ref. [25], the systematic use of the MWCM is seen to result in about 95% of the estimates falling within an error interval equal to ±15%: this fully proves that the MWCM is a powerful engineering tool suitable for designing engineering materials against multiaxial fatigue.

REFERENCES

[1] H. J. Gough, In: Proceedings of the Institution of Mechanical Engineers, 160 (1949) 417.
[2] K. Dang Van, B. Griveau, O. Messagge, In: Biaxial and Multiaxial Fatigue, EGF 3, Edited by M. W. Brown and K. J. Miller, Mechanical Engineering Publications, London, (1989) 479.
[3] I. V. Papadopoulos, Fatigue polycyclique des métaux: une novelle approche. Thèse de Doctorat, Ecole Nationale des Ponts et Chaussées, Paris, France (1987).
[4] G. Sines, In: Metal Fatigue, Edited by G. Sines and J. L. Waisman, McGraw-Hill, New York, (1959) 145.
[5] B. Crossland, In: Proceedings of the International Conference on Fatigue of Metals, Institution of Mechanical Engineers, London, (1956) 138.
[6] E. N. Mamiya, J. A. Araújo, F.C. Castro, Int. J. Fatigue, 31 (2009) 1144.
[7] T. Matake, Bulletin of the JSME 20 141 (1977) 257.
[8] D. L. McDiarmid, Fatigue & Fracture of Engineering Materials & Structures, 14 (1991) 429.
[9] A. Carpinteri, R. Brighenti, A. Spagnoli, Fatigue & Fracture of Engineering Materials and Structures, 23 (2000) 355.
[10] K. Kanazawa, K. J. Miller, M. W. Brown, Transactions of the ASME, Journal of Engineering Materials and Technology, July (1977) 222.
[11] L. Susmel, Multiaxial Notch Fatigue: from nominal to local stress-strain quantities. Woodhead & CRC, Cambridge, UK, ISBN: 1 84569 582 8, (2009).
[12] L. Susmel, P. Lazzarin, Fatigue & Fracture of Engineering Materials & Structures, 25 (2002) 63.
[13] L. Susmel, Fatigue & Fracture of Engineering Materials & Structures, 31 (2008) 295.
[14] L. Susmel, N. Petrone, In: Biaxial and Multiaxial fatigue and Fracture, Edited by A. Carpinteri, M. de Freitas and A. Spagnoli, Elsevier and ESIS, (2003) 83.
[15] P. Lazzarin, L. Susmel, Fatigue & Fracture of Engineering Materials and Structures, 26 (2003) 1171.
[16] L. Susmel, D. Taylor, Fatigue & Fracture of Engineering Materials & Structures, 26 (2003) 821.
[17] L. Susmel, Fatigue & Fracture of Engineering Materials & Structures, 27 (2004) 391.
[18] L. Susmel, D. Taylor, International Journal of Fatigue, 28 (2006) 417.
[19] L. Susmel, D. Taylor, Fatigue & Fracture of Engineering Materials & Structures, 31(12) (2008) 1047.
[20] L. Susmel, R. Tovo, Fatigue & Fracture of Engineering Materials & Structures, 27 (2004) 1005.
[21] L. Susmel, R. Tovo, International Journal of Fatigue, 28 (2006) 564.
[22] L. Susmel, International Journal of Fatigue, 30 (2008) 888.
[23] L. Susmel, International Journal of Fatigue, 31 (2009) 197.
[24] L. Susmel, International Journal of Fatigue, 32 (2010) 1057.
[25] J. Papuga, International Journal of Fatigue, 33 (2011) 153.
[26] L. Susmel, R. Tovo, P. Lazzarin, International Journal of Fatigue 27 (2005) 928.
[27] R. P. Kaufman, T. Topper, In: Biaxial and Multiaxial fatigue and Fracture, Edited by A. Carpinteri, M. de Freitas and A. Spagnoli, Elsevier and ESIS, (2003) 123.
[28] L. Susmel, International Journal of Fatigue, 32 (2010) 1875.
[29] D. F. Socie, Transactions of the ASME, Journal of Engineering Materials and Technology, 109 (1987) 293.
[30] H. J. Gough, H. V.Pollard, W. J. Clenshaw, Some experiments on the resistance of metals to fatigue under combined stresses. Aeronautical Research Council, R and M 2522. HMSO, London (1951).
[31] H. J. Gough, H. V. Pollard, In: Proceedings of Institute of Mechanical Engineering, 131 (1935) 1.
[32] P. H. Frith, In: Proceedings of the Institution of Mechanical Engineers, (1956) 462.
[33] W. N. Findley, J. J. Coleman, B. C. Hanley, In: Proceedings of International Conference on Fatigue of Metals, Institution of Mechanical Engineers, London, (1956) 150.
[34] T. Nishihara, M. Kawamoto, Memoirs of the College of Engineering, Kyoto Imperial University 10, (1941) 177.
[35] S. Kitaioka, J. Chen, M. Seika, Bulletin of the Japan Society of Mechanical Engineers, 29 (1986) 214.
[36] C. Froustey, Fatigue multiaxiale en endurance de l'acier 30NCD16, PhD Thesis, Ecole Nationale Supérieure d'Arts et Métiers, Bordeaux, France(1987).
[37] C. Froustey, S. Lasserre, International Journal of Fatigue, 11 (1989) 169.

[38] M. Ros, Die Bruchegefahr fester Koper. EMPA Bericht 173, Zurich, Germany (1950).
[39] F. Rotvel, International Journal of Mechanical Science, 12 (1970) 597.
[40] T. Nishihara, M. Kawamoto, Memoirs of the College of Engineering, Kyoto Imperial University, 11 (1945) 85.
[41] H. Zenner, R. Heidenreich, I. Richter, Dauerschwingfestigkeit bei nichtsynchroner mehrachsiger beanspruchung. Z. Werkstofftechnik, 16 (1985) 101.
[42] W. Lempp, Festigkeitsverhalten von Stählen bei mehrachsiger Dauerscwingbeanspruchung durch Normalspannungen mit überlagerten phasengleichen und phasenverschobenen Schubspannungen. Dissertation, University of Stuttgart, Germany (1977).
[43] L. Issler, Festigkeitsverhalten metallischer Wekstoffe bei mehrachsiger phasenverschobener Schwingbeanspruchung. Dissertation, Universität Stuttgard, Germany (1973).
[44] J. Liu Beitrag zur Verbesserung der Dauerfestigkeitsberechnung bei mehrachsiger Beanspruchung. Dissertation, TU Clausthal; Germany (1991).
[45] D. L. McDiarmid, In: Multiaxial Fatigue, Edited by K. J. Miller and M. W. Brown, ASTM STP 853, (1985) 606.
[46] C. Froustey, S. Lasserre, L. Dubar, In: Proceedings of MET-TECH 92, Grenoble, France (1992).
[47] C. Kaniut, Zur Betriebsfestigkeit metallischer Werstoffe bei mehrashsiger Beanspruchunng. Diss RWTH, Aachen, Germany (1983).
[48] M. Fougé, J. Bahuaud, In : Proceedings of Comptes Rendus 7ème Congrès Français de Mecanique, Bordeaux, France, (1985) 30.
[49] S. Mielke, Festigkeitsverhalten metallischer Werkstoffe unter zweiachsiger schwingender Beanspruchung mit verschiedenen Spannungszeitverlaeufen. PhD thesis, RWTH Aachen (1980).
[50] H. Achtelik, I. J akubowska, E. Macha, Studia Geotechnica et Mechanica, V 2 (1983) 9.
[51] A. Simbürger, Festigkeitverhalten zähler Werkstoffe bei einer Mehrachsigen, Phasenverscobenen Schwingbeanspruchung mit Köroperfesten Hauptspannungsrichtungen. LBF Bericht Nr. FB-121, Darmstad, Germany (1975).
[52] T. Palin-Luc, S. Lasserre, European Journal of Mechanics - A/Solids, 17 (1998) 237.
[53] C. M. Sonsino, International Journal of Fatigue, 17 (1995) 55.
[54] R. Akrache, J. Lu, Fatigue and Fracture of Engineering Materials & Structures, 22 (1999) 527.
[55] T. Delahay, T.Palin-Luc, International Journal of Fatigue, 28 (2006) 474.
[56] H. Altenbach, A. Zolochevsky, Fatigue and Fracture of Engineering Materials & Structures, 19 (1996) 1207.
[57] A. Bernasconi, M. Filippini, S. Foletti, D. Vaudo, International Journal of Fatigue, 28 (2006) 663.
[58] J. Froeschl, G. Gerstmayr, W. Eichlseder, H. Leitner, In: Proceedings of 8th International Conference on Multiaxial Fatigue and Fracture, Edited by U. S. Fernando, Sheffield, UK, (2007) S3-1.
[59] Bernasconi, M. Foletti, I. V. Papadopoulos, International Journal of Fatigue, 30 (2008) 1430.
[60] H. Bomas, S. Kunow, G. Loewisch, R. Kienzler, R. Schroeder, M. Bacher-Hoechst, F. Muehleder, In: Proceedings of Fatigue 2006 Conference. Ed: Johnson, W. S. Oxford, Elsevier Ltd, (2006).
[61] L. Dubar, Fatigue multiaxiale des aciers. Passage de l'endurance a l'endurance limite. Prise en compte des accidents geometriques. PhD thesis, Talence, ENSAM (1992).
[62] R. Heidenreich, H. Zenner, Schubspannungsintensitaetshypothese - Erweiterung und experimentelle Abschaetzung einer neuen Festigkeitshypothese fuer schwingende Beanspruchung. Technical report Forschungshefte FKM, Heft 77, Frankfurt am Main – Niederrad (1979).
[63] E. El Magd, S. Mielke, Konstruktion, 29(7) (1977) 253.
[64] W. N. Findley, Combined-stress fatigue strength of 76S-T61 aluminum alloy with superimposed mean stresses and corrections for yielding. Technical report NACA TN-2924, Washington, USA (1953).
[65] A. Troost, O. Akin, F. Klubberg, Konstruktion, 39 (1987) 479.
[66] F. Nolte, Dauerfestigkeitsuntersuchungen an Stahlwellen bei umlaufender Beige- und überlagerter statischer Verdrehbeanspruchung. PhD Thesis, TU Berlin, Germany (1973).
[67] B. Paysan, Untersuchungen des Einflusses einiger Kerbformen auf die Tragfähigkeit von Wellen bei umlaufender biegung und überlagerter überlagerter statischer torsion. PhD Thesis, TU Berlin, Germany (1970).
[68] V. Papadopoulos, Fatigue & Fracture of Engineering Materials & Structures, 18 (1995) 79.
[69] Z. Gao, B. Qiu, X. Wang, Y. Jiang, International Journal of Fatigue, 32 (2010) 1960.
[70] P. Kurath, S. D. Downing, D. R. Galliart, In: Multiaxial Fatigue - Analysis and Experiments. Edited by G.E. Leese and D. F. Socie, SAE AE-14 (1989) 13.
[71] B. Atzori, F. Berto, P. Lazzarin, M. Quaresimin, International Journal of Fatigue, 28 (2006) 485.

[72] G. Quilafku, N. Kadi, J. Dobranski, Z. Azari, M. Gjonaj, G. Pluvinage, International Journal of Fatigue, 23 (2001) 689.
[73] R. E. Peterson, In: Metal Fatigue, Edited by G. Sines and J. L. Waisman, McGraw Hill, New York, (1959) 293.
[74] Y.-L. Lee, J. Pan, R. B. Hathaway, M. E. Barkey Fatigue Testing and Analysis. Elsevier Butterworth–Heinemann. ISBN 0-7506-7719-8 (2005).